

Thermal conductivity studies on ceramic floor tiles

E. García^a, A. de Pablos^a, M.A. Bengoechea^b, L. Guaita^b, M.I. Osendi^a, P. Miranzo^{a,*}

^a*Institute of Ceramics and Glass (ICV), CSIC, Madrid, Spain*

^b*Keraben Grupo, S.A., Nules, Castellón, Spain*

Received 16 June 2010; received in revised form 27 July 2010; accepted 1 September 2010

Available online 29 September 2010

Abstract

Thermal diffusivity, thermal conductivity and specific heat of several materials used as floor tiles have been measured using the laser flash method. Natural stones, particularly granite, porcelain stoneware and red stoneware materials of low water absorption, are more effective thermal conductors than white stoneware and vinyl, which have thermal conductivities below $1 \text{ W m}^{-1} \text{ K}^{-1}$. Therefore, last two should not be recommended for radiant floor heating applications. Enhancement of thermal conductivity of red and porcelain stoneware has been achieved by adding Al_2O_3 of certain characteristics to the ceramic paste. In this way, thermal diffusivity increases of up to 50% have been obtained by adding 20 wt.% of Al_2O_3 particles.

© 2010 Elsevier Ltd and Techna Group S.r.l. All rights reserved.

Keywords: Thermal properties; Thermal conductivity; Stoneware tiles; Traditional ceramics; Al_2O_3

1. Introduction

Nowadays there is a growing trend in using the radiant floor heating system for domestic applications, being one of the more widely used heating systems in northern Europe countries [1]. These systems directly supply heat to the floor and largely depend on the effective heat transfer from the hot surface to the people and objects in the room. Despite the name, radiant floor heating systems also depend heavily on convection, i.e. the natural circulation of heat within a room, caused by heat rising from the floor. Either electric wiring [2] or a tubing system, placed directly under a tiled floor or embedded in concrete below the tiled floor, transporting hot water [3,4] (hydronic radiant floors) or air [5] heated up to 70°C , are used to warm rooms up to 28°C [6]. The radiant floor heating system is an efficient way to obtain thermal comfort in buildings as it warms objects, furniture and people, instead of heating air and circulating it throughout the house. Although it depends on the application, it is usually admitted that radiant heating systems are 20–40% more energy efficient than other conventional heating systems.

Computer simulations [7–9] about the effect of several designing parameters on the floor heating system performance have concluded that the most important factors are the floor material type and thickness. The floor tile is critical as it determines the energy transfer capability; anything that can insulate the floor also limits heat entering the space from the floor heating system, increasing fuel consumption. Ceramic tiles may be effective floor coverings for radiant floor heating because they are good thermal conductors compared to other floor coverings like carpets or vinyl, also adding the benefit of their thermal storage capability owing to their high heat capacity [10]. Among the ceramic covering floors, stoneware materials are universally considered as the best candidates because they do not deform under temperature changes and offer an advantageous benefits/cost ratio. A lot of works can be found in the literature about the processing of ceramic tile materials [11–14], the viability of different raw materials [15–20] and new trends [21,22]. However, their technical properties have been scarcely studied, being mainly focused on the mechanical properties [23–25]. To the extent of our knowledge, there are limited studies on the thermal properties of clay based materials [26,27], and even less, of ceramic tiles [28].

In the present work, the thermal properties of different floor covering materials suitable for radiant floor heating systems are analysed in terms of their thermal diffusivity, specific heat and thermal conductivity. In this way, a data base of materials

* Corresponding author at: Instituto de Ceramica y Vidrio, CSIC, Kelsen 5, 28049 Madrid, Spain. Tel.: +34 917355872; fax: +34 917355843.

E-mail address: pmiranzo@icv.csic.es (P. Miranzo).

measured under similar conditions that can be useful for scientists and professionals of the floor tile market is provided. Furthermore, with the aim of enhancing the thermal efficiency of stoneware ceramic tiles, compositions of two selected tiles were modified by adding a second phase of higher thermal conductivity like alumina. Results of these modifications are comparatively addressed focussing on the thermal conductivity enhancement.

2. Experimental

The different commercial tiles considered for this study are shown in Table 1, grouped as natural stone (NT) tiles (marble, granite and terrazzo), plastic tiles as vinyl, and ceramic tiles, which may be further divided into red and white stoneware (S) and porcelain stoneware (PS). Differences between the last two are mainly due to the higher firing temperatures used for PS tiles that lead to higher densities, compared to the S tiles. Commercial PS and S with different degree of densification have been considered for the study.

Thermal diffusivity and specific heat were measured as a function of temperature up to 250 °C by the laser-flash method (Thermaflash 2000, Netzsch-Holometrix, USA, standard E 1461-1992), using disc specimens of 12.7 mm in diameter and 1 mm in thickness machined from the different tiles. The surfaces of the specimens were gold and graphite coated to prevent the laser transmission and to ensure a good absorption of the IR energy. A Pyrex standard of same dimensions was used as reference for the specific heat measurements, as it has thermal diffusivity and specific heat similar to the floor tile ceramic materials. The software of the equipment allows analyzing the signal using different approximations that take into account the heat losses. The Taylor approach [29] was used in this work to consider radial heat losses that usually take place when testing low thermal diffusivity materials. Data at each temperature is averaged over three measurements. The thermal diffusivity (α) of the materials is given with an accuracy of 5%, whereas the accuracy of the equipment for specific heat calculation is around $\approx 7\%$. From thermal diffusivity and specific heat values, the thermal conductivity was calculated through the expression:

$$K = \alpha C_p \rho \quad (1)$$

using the density of the samples measured by water immersion methods.

For the modified compositions of the S and PS tiles, two types of α -Al₂O₃ powders with mean particle size (d_{50}) of 4 μ m and 0.5 μ m, respectively, and γ -Al₂O₃ powders of $d_{50} = 96 \mu$ m were chosen as additions (Table 2). Those alumina powders

Table 1

Commercial tile materials studied in the present work.

Group	Material	Density (g cm ⁻³)
Natural stone (NT)	Pink marble	2.70
	Terrazzo	2.58
	Granite	2.87
Plastic	Vinyl	1.20
Stoneware tiles		
Porcelain (PS)	Polished black	2.38
	Polished white	2.41
Red (red-S)	Porous	1.98
	High water abs.	2.23
	Low water abs.	2.31
White (white-S)	Porous	1.67
	High water abs.	2.10
	Low water abs.	2.31

were added in a percentage of 20 wt.% to corresponding batches of red-S and PS slurries (63 wt.% of solid contents) and slurries were ball milled for 1 h to get good homogeneity. Subsequently, slurries were spray-dried. Granules were humidified by adding 5 wt.% of water and uniaxially pressed at 25 MPa using a 60 mm \times 60 mm square die. After demoulding, green specimens of 60 mm \times 60 mm \times 10 mm were obtained. The modified compositions were sintered at temperatures between 1120 and 1160 °C for red-S based ceramics and between 1160 and 1200 °C for the PS based materials. Crystalline phases in the original and modified tiles were analysed by X-ray diffraction (XRD) methods in powdered samples. The microstructure was viewed by reflected light optical microscopy on specimens after polishing and acid etching by immersion in a HF acid solution (10 vol.%). For higher magnification observation and phase adscription, scanning electron microscopy (SEM) together with energy dispersive X-ray spectroscopy (EDS) analysis were used.

3. Results and discussion

3.1. Commercial tile materials

Density values obtained by the water immersion method are shown in Table 1. Among the natural materials, granite showed the highest density, the values were consistently higher for PS materials than for S (red or white) tiles, and vinyl tile had the lowest density of all. Representative optical images of the microstructure of natural stone and stoneware tiles are shown in Fig. 1. As shown in Table 3, the granite tile contains quartz, feldspars and muscovite mica (H₂KAl₃Si₃O₁₂) and exhibited very low porosity (Fig. 1a). The ceramic tiles (Fig. 1b and c) showed more porosity and quartz as the major phase, as it is

Table 2
Characteristics of the alumina powders employed as additives for the stoneware materials.

Label	Company	Product	Phase	Purity (%)	Agglomerate mean size (μ m)
0.5A	ALCOA Ind. Chemical (USA)	CT 3000 SG	α	99.85	0.5
4A	Aluminio Español S.A. (Spain)	SC B/01-D	α	99.6	4.0
γ -Al ₂ O ₃		SC-0	γ	≥ 98	96.0

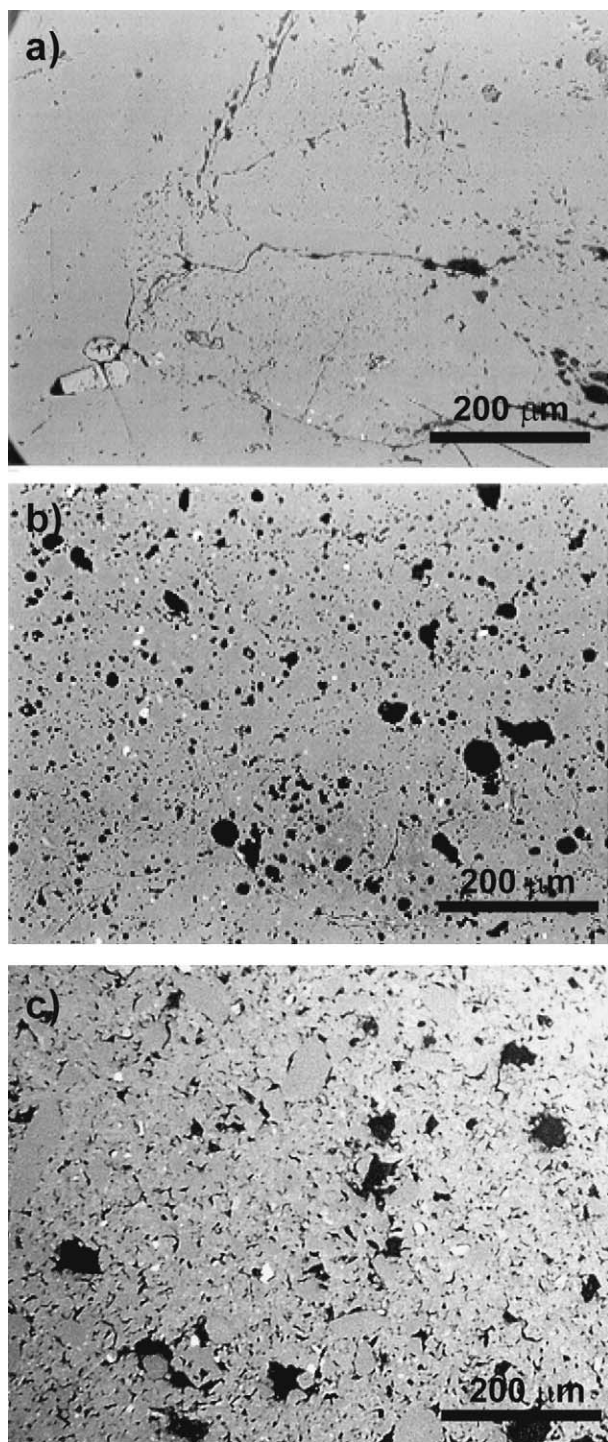


Fig. 1. MORL micrographs of various tile materials: (a) granite, (b) PS and (c) red-S.

usual in porcelain and stoneware materials. Besides, PS material had traces of mullite ($3\text{Al}_2\text{O}_3 \cdot 2\text{SiO}_2$) and albite ($\text{NaAlSi}_3\text{O}_8$); whereas for red-S and white-S materials, hematite (Fe_2O_3) and albite ($\text{NaAlSi}_3\text{O}_8$), respectively, were identified.

The thermal diffusivity data for commercial materials are plotted as a function of temperature in Fig. 2, indicating that vinyl material had the lowest thermal diffusivity, as low as

Table 3

Summary of the XRD results for granite and stoneware ceramic tiles.

	Components
Granite	<i>Feldspars</i> : Microcline (KAlSi_3O_8) Anorthite ($\text{CaAl}_2(\text{SiO}_4)_2/(\text{CaO} \cdot \text{Al}_2\text{O}_3 \cdot 2\text{SiO}_2)$) Albite ($\text{NaAlSi}_3\text{O}_8$) <i>Mica</i> : Muscovite ($\text{H}_2\text{KAl}_3\text{Si}_3\text{O}_{12}$) Quartz (SiO_2)
Stoneware	
PS	Quartz (SiO_2) Mullite ($3\text{Al}_2\text{O}_3 \cdot 2\text{SiO}_2$) <i>Feldspars</i> : Albite ($\text{NaAlSi}_3\text{O}_8$)
White-S	Quartz (SiO_2) <i>Feldspars</i> : Albite ($\text{NaAlSi}_3\text{O}_8$)
Red-S	Quartz (SiO_2) Hematite (Fe_2O_3)

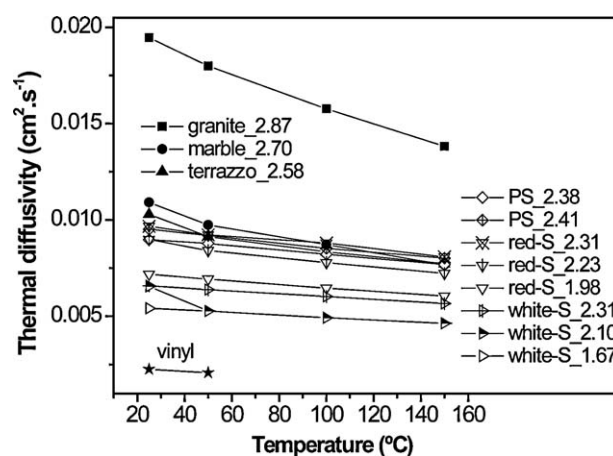


Fig. 2. Thermal diffusivity (α) as a function of temperature of the floor tile materials given in Table 1. The label numbers indicate the densities in g cm^{-3} .

$0.0025 \text{ cm}^2 \text{ s}^{-1}$, and granite tile, the highest, more than twice higher than the rest. The thermal diffusivities of the S and PS tiles were in the range $0.005\text{--}0.010 \text{ cm}^2 \text{ s}^{-1}$ and they seem to correlate with the density values, which are included in the label of each material in Fig. 2. The slightly higher values obtained for the red-S tiles compared to the white-S materials of same density can be related to the higher amount of hematite in the first.

As seen in Fig. 3, room temperature specific heat values were in the range $0.65\text{--}0.95 \text{ J g}^{-1} \text{ K}^{-1}$. Room temperature estimations of C_p by the laser flash method had low precision because the high noise/signal ratio, although less dispersion was observed at temperatures above 50°C . In the case of the natural stone tiles, the room temperature C_p data was extrapolated from the value at 50°C . Besides, C_p deviations of 10% and 4% were seen after 10 different tests on ceramic tiles done at room temperature and 100°C , respectively.

Introducing data from Figs. 2 and 3, and the density of each material in Eq. (1), thermal conductivity values plotted in Fig. 4a were calculated. Floor tile materials studied in this work presented a wide range of thermal conductivities, framed by the low thermal conductivity of vinyl (below $0.20 \text{ W m}^{-1} \text{ K}^{-1}$) and the upper limit of granite ($4 \text{ W m}^{-1} \text{ K}^{-1}$). The thermal

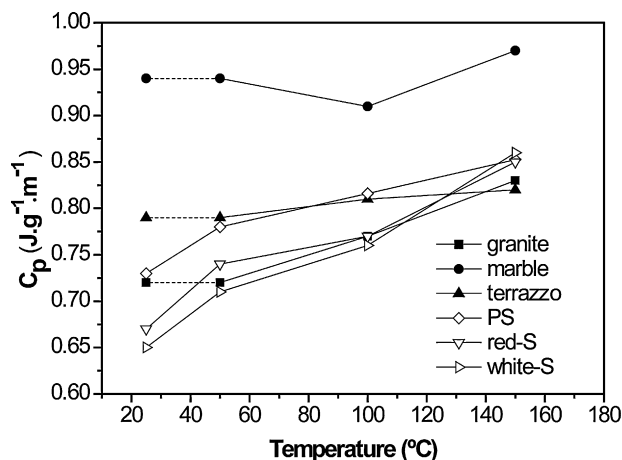


Fig. 3. Specific heat (C_p) as a function of temperature for the floor tile materials given in Table 1.

conductivity of the ceramic tile materials at room temperature, which varied from 0.6 to $1.7 \text{ W m}^{-1} \text{ K}^{-1}$, correlates to their density as shown in Fig. 4b. The higher Fe_2O_3 content [30] of the red-S ceramics may explain its higher thermal conductivity compared to the white-S tiles of similar densities. The presence of crystalline phases such as mullite, with typical thermal

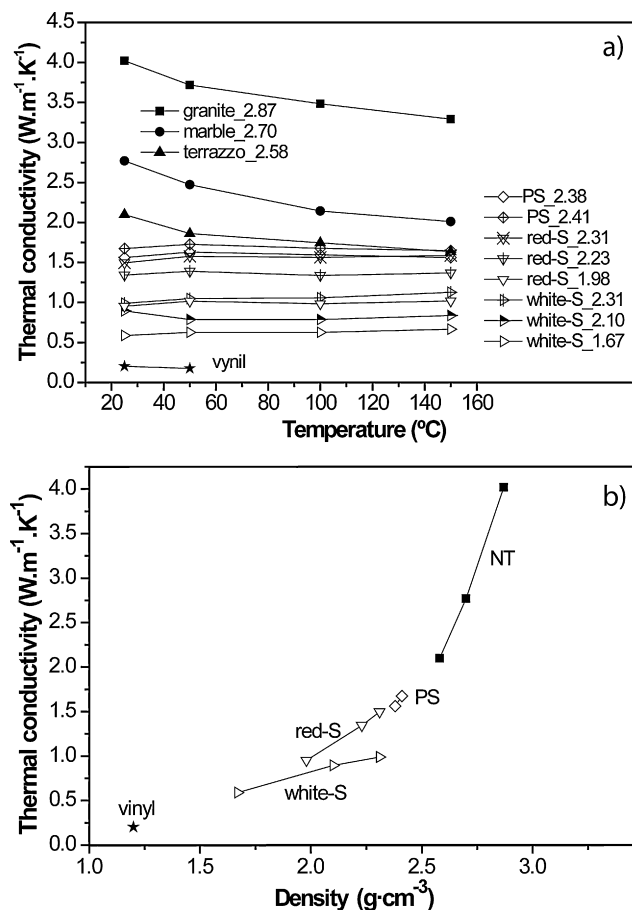


Fig. 4. (a) Thermal conductivity (K) as a function of temperature for the floor tile materials given in Table 1. The label numbers indicate the densities in g cm^{-3} . Values at room temperature as a function of density are plotted in (b).

Table 4

Firing temperatures and water absorption data for alumina modified stoneware tiles. Figures for blank materials are given for comparison. The thermal conductivity was measured for the highlighted specimens.

	Firing temperature ($^{\circ}\text{C}$)	Water absorption (wt.%)
Red-S		
Blank	1120	5.7
0.5A	1120	7.8
	1140	4.9
	1160	3.7
4A	1120	10.3
	1140	6.4
	1160	5.8
$\gamma\text{-Al}_2\text{O}_3$	1120	16.4
	1140	15.2
	1160	13.8
PS		
Blank	1160	5.3
4A	1160	10.4
	1180	7.3
	1200	5.5
$\gamma\text{-Al}_2\text{O}_3$	1160	16.3
	1180	13.0
	1200	11.0

conductivity of $5 \text{ W m}^{-1} \text{ K}^{-1}$ at room temperature [31], could also contribute to the higher value of thermal conductivity exhibited by PS tile materials.

3.2. Modified stoneware materials: effect of a high conducting Al_2O_3 phase

The addition of Al_2O_3 had a strong influence on densification of the stoneware materials, PS and red-S (Table 4). The blank red-S was fired at 1120°C , had $\sim 5\%$ of water absorption and did not show massive vitrification. On the other hand, for a blank PS material of similar water absorption a firing temperature of 1160°C was used. When adding Al_2O_3 particles, densification was retarded and a rise in the sintering temperature was required to get comparable porosities, this effect being more pronounced as the Al_2O_3 particle size increased. In particular, at least 20°C higher firing temperatures (1140 and 1160°C) were needed for red-S materials to get similar water absorption as the blank when adding $\alpha\text{-Al}_2\text{O}_3$ particles of 0.5 and $4 \mu\text{m}$, respectively. Furthermore, water absorptions lower than 14% could not be reached when $\gamma\text{-Al}_2\text{O}_3$ powders of $96 \mu\text{m}$ were used, at any firing temperature. Similar results were obtained for the PS material; firing temperatures around 1200°C were required to get 5% of water absorption for 4A $\alpha\text{-Al}_2\text{O}_3$ addition, whereas open porosity values higher than 11% were obtained at any firing temperature for the $\gamma\text{-Al}_2\text{O}_3$.

Fig. 5 shows the XRD patterns of all the stoneware materials before and after the Al_2O_3 additions. In the case of the red-S material (Fig. 5a) just extra $\alpha\text{-Al}_2\text{O}_3$ peaks were detected. However, in the PS material (Fig. 5b), the albite existing in the blank specimen nearly disappeared while $\alpha\text{-Al}_2\text{O}_3$ peaks emerged. The SEM comparison of these four materials is shown in Fig. 6 with identification of the main phases in the

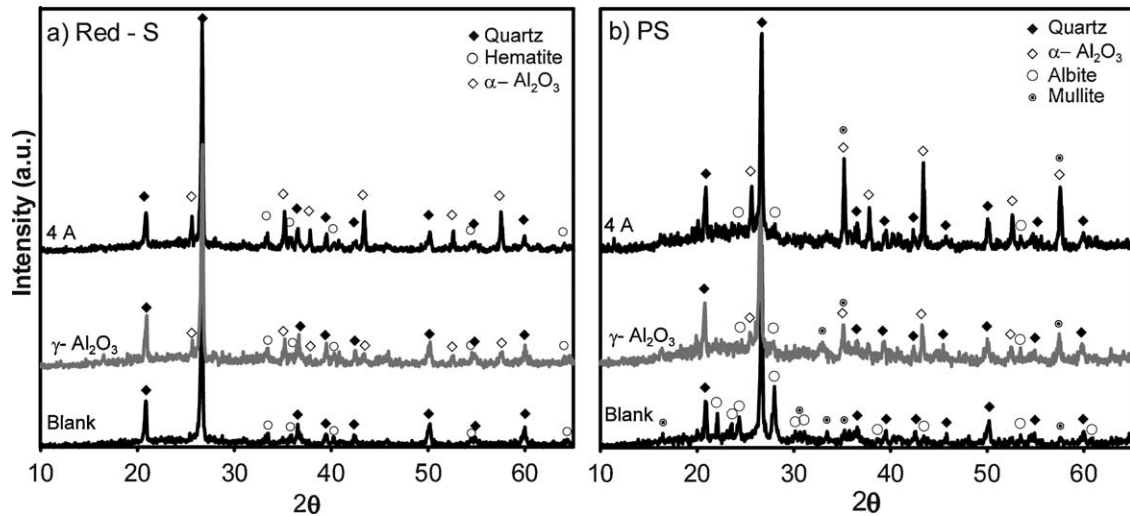


Fig. 5. XRD patterns of (a) red-S and (b) PS materials: data for blank and the corresponding materials modified with 20 wt.% of Al_2O_3 are presented.

micrographs, considering information from EDS and XRD analyses. Significant microstructural differences were not observed in the red-S materials (Fig. 6a and c); whereas extended glassy formation was observed in the PS materials when Al_2O_3 was added (Fig. 6b and d). In line with the albite

vanishing detected by XRD, there was a glassy phase boost linked to albite grains dissolving in the matrix (Fig. 6d) due to the higher firing temperature, $>1180^\circ\text{C}$ (Table 4).

The effect of $\alpha\text{-Al}_2\text{O}_3$ addition on the thermal diffusivity/conductivity was analysed by comparing data at 25 and 100°C

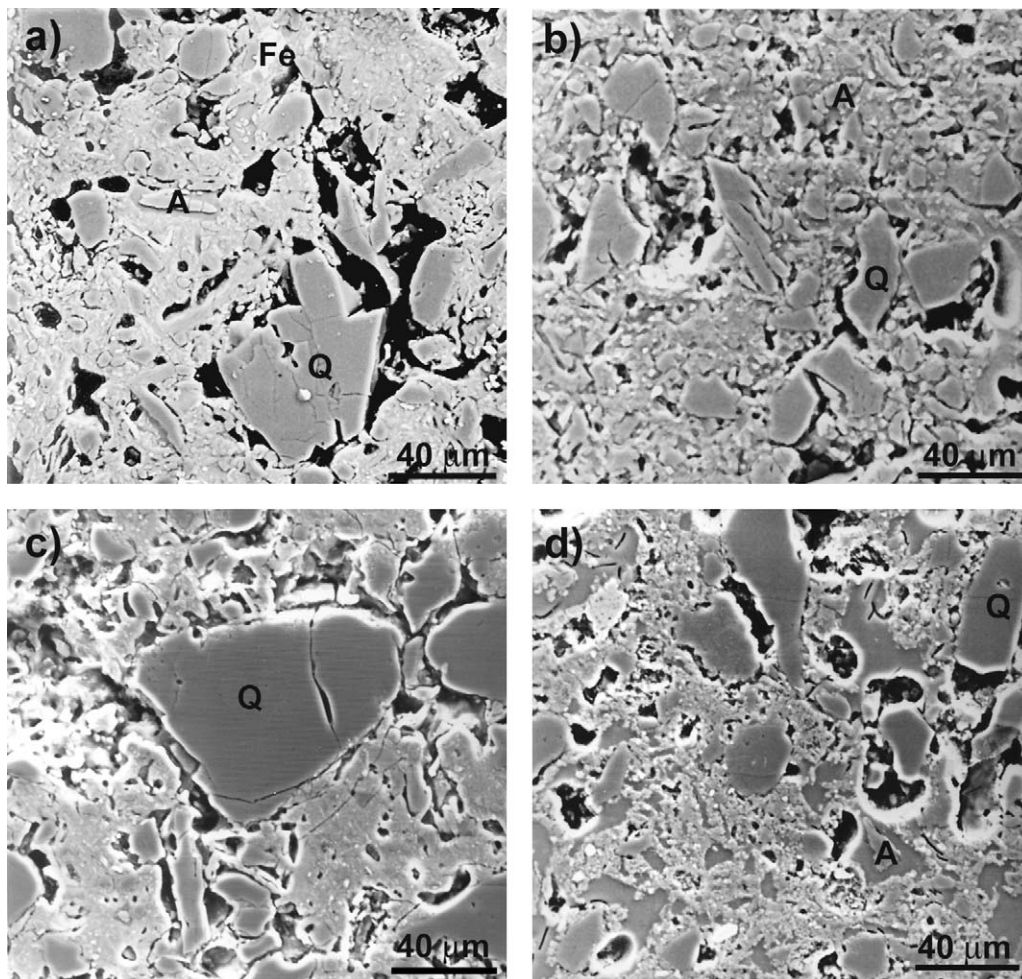


Fig. 6. SEM micrographs of (a) red-S, (b) PS, (c) red-S-4A and (d) PS-4A materials, where Q, quartz; A, albite and Fe, Fe_2O_3 .

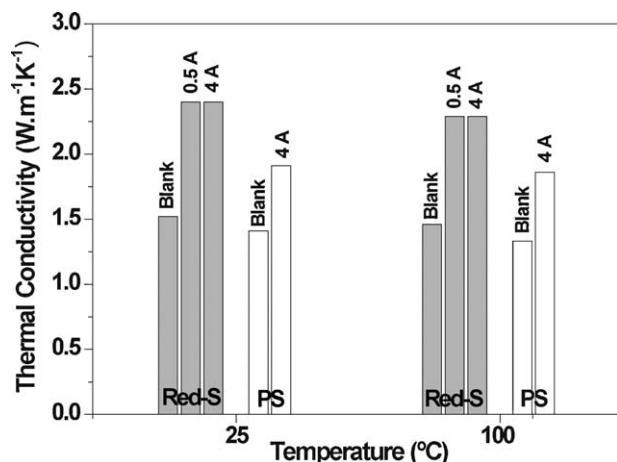


Fig. 7. Thermal conductivity at 25 and 100 °C for red-S and PS materials: blank and modified with 20 wt.% of 4A and 0.5A α - Al_2O_3 powders.

of selected PS and red-S specimens all having a similar open porosity of $\sim 5\%$ (Fig. 7) in order to avoid the effect of this parameter on the thermal behaviour. The specimens studied are grey highlighted in Table 4. Al_2O_3 addition increased the thermal diffusivity and conductivity of both tile materials, being the specific heat values in the range $0.7\text{--}0.9 \text{ J g}^{-1} \text{ K}^{-1}$ in all cases. As seen in Fig. 7, the thermal conductivity of the PS-4A was 35% higher than that of the blank PS material and the increment was even more dramatic (50%) for the red-S-4A and red-S-0.5A modified materials. Results were practically indifferent of the type of α - Al_2O_3 used as additive, when considering materials of similar density. This thermal conductivity enhancement is mainly due to the high thermal conductivity of the Al_2O_3 phase, 28.2 and $21.9 \text{ W m}^{-1} \text{ K}^{-1}$ at room temperature and 100 °C, respectively, for a dense alumina [32]. The different increase found for the both types of stoneware materials, higher in the case of S than in PS, can be caused by the larger amount of glassy phase that formed in PS material with the alumina addition (Fig. 6d).

An estimation of the thermal conductivity can be done using the well known Eucken's equation [33] considering that modified materials are composites formed by a matrix, whose thermal conductivity is that of the corresponding blank stoneware, and a dispersed Al_2O_3 phase with thermal conductivity of $28.2 \text{ W m}^{-1} \text{ K}^{-1}$. The volume fraction of Al_2O_3 was 0.13, calculated from the weight percentage of Al_2O_3 added (20 wt.%), the density of the blank material and the theoretical density of Al_2O_3 (3.97 g cm^{-3}). In this way, a value of $2.1 \text{ W m}^{-1} \text{ K}^{-1}$ is predicted for the modified materials. As the measured values for modified red-S materials are higher ($2.4 \text{ W m}^{-1} \text{ K}^{-1}$) than the predicted, we can infer that Al_2O_3 was percolated for both 4A and 0.5A powders, which explains that thermal conductivity did not depend on the Al_2O_3 particle size.

4. Summary

Granite is the most effective thermal conductor among the floor tiles analysed. Terrazzo, marble, porcelain stoneware and red stoneware of low water absorption have thermal

conductivities above $1 \text{ W m}^{-1} \text{ K}^{-1}$. White stoneware materials and vinyl have values below $1 \text{ W m}^{-1} \text{ K}^{-1}$, therefore should not be recommended for radiant floor heating applications.

By an adequate selection of the firing temperature, the addition of Al_2O_3 (20 wt.%) allows increasing the thermal conductivity of red (up to 50%) and porcelain stoneware (35%) materials, avoiding significant alterations of the porosity and microstructure and approaching the value of K to that of marble. The porcelain stoneware materials present a smaller increment because the higher firing temperature required for achieving same porosity produces significant amount of glassy phase.

Acknowledgements

The financial support of KERABEN GRUPO, S.A. and MAT 2009-09600 is recognized. Eugenio Garcia acknowledges the Ramón y Cajal Program for his financial support.

References

- [1] B.W. Olesen, M. Koschenz, C. Johanson, New European standard proposal for design and dimensioning of embedded radiant surface heating and cooling systems, *ASHRAE Trans.* 109 (2003) 656–668.
- [2] K. Lin, Y. Zhang, X. Xu, H. Di, R. Yang, P. Qin, Experimental study of under-floor electric heating system with shape-stabilized PCM plates, *Energy Build.* 37 (3) (2005) 215–220.
- [3] B.W. Olesen, Radiant floor heating in theory and practice, *ASHRAE J.* 44 (7) (2002) 19–26.
- [4] M. De Carli, B.W. Olesen, Field measurements of operative temperatures in buildings heated or cooled by embedded water-based radiant systems, *ASHRAE Trans.* 108 (2) (2002) 714–725.
- [5] O. Bozkir, S. Canbazoglu, Unsteady thermal performance analysis of a room with serial and parallel duct radiant floor heating system using hot airflow, *Energy Build.* 36 (2004) 579–586.
- [6] ASHRAE Handbook – Heating, Ventilating, and Air-Conditioning Applications (I-P Edition) American Society of Heating, Refrigerating and Air-Conditioning Engineers, Inc., 2007.
- [7] K. Lin, Y. Zhang, X. Xu, H. Di, R. Yang, P. Qin, Modeling and simulation of under-floor electric heating system with shape-stabilized PCM plates, *Build. Environ.* 39 (12) (2004) 1427–1434.
- [8] S.H. Cho, M. Zaheer-Uddin, Predictive control of intermittently operated radiant floor heating systems, *Energy Convers. Manage.* 44 (2003) 1333–1342.
- [9] S. Sattari, B. Farhanieh, A parametric study on radiant floor heating system performance, *Renew. Energy* 31 (2006) 1617–1626.
- [10] Ceramics and Glasses, in: S.J. Schneider (Ed.), *Engineering Materials Handbook*, vol. 4, ASM International, 1991.
- [11] E. Sánchez, Technical considerations on porcelain tile products and their manufacturing process. Part I, *Interceram* 52 (1) (2003) 6–16.
- [12] E. Sánchez, Technical considerations on porcelain tile products and their manufacturing process, Part II, *Interceram* 52 (3) (2003) 132–138.
- [13] J.R. Martí, A. Sanchez, Dry grinding process for the preparation of floor & wall tile bodies, *Interceram: Int. Ceram. Rev.* 58 (4) (2009) 213–215.
- [14] M.J. Orts, A. Escardino, J.L. Amoros, F. Negre, Microstructural changes during the firing of stoneware floor tiles, *Appl. Clay Sci.* 8 (1993) 193–205.
- [15] P.R. Torres, S. Manjate, S. Quaresma, H.R. Fernandes, J.M.F. Ferreira, Development of ceramic floor tile compositions based on quartzite and granite sludges, *J. Eur. Ceram. Soc.* 27 (2007) 4649–4655.
- [16] R. Sokolar, L. Smetanova, Dry pressed ceramic tiles based on fly ash-clay body: influence of fly ash granulometry and pentasodium triphosphate addition, *Ceram. Int.* 36 (2010) 215–221.

- [17] M.A. Montero, M.M. Jordán, M.S. Hernández-Crespo, T. Sanfeliu, The use of sewage sludge and marble residues in the manufacture of ceramic tile bodies, *Appl. Clay Sci.* 46 (4) (2009) 404–408.
- [18] M.A. Montero, M.M. Jordán, M.B. Almendro-Candel, T. Sanfeliu, M.S. Hernández-Crespo, The use of a calcium carbonate residue from the stone industry in manufacturing of ceramic tile bodies, *Appl. Clay Sci.* 43 (2) (2009) 186–189.
- [19] A.P. Luz, S. Ribeiro, Use of glass waste as a raw material in porcelain stoneware tile mixtures, *Ceram. Int.* 33 (2007) 761–765.
- [20] E. Rambaldi, L. Esposito, A. Tucci, G. Timellini, Recycling of polishing porcelain stoneware residues in ceramic tiles, *J. Eur. Ceram. Soc.* 27 (2007) 3509–3515.
- [21] G. Nassett, Technological and productive innovations in the ceramic industry with particular reference to ceramic floor and wall tiles, *Mater. Sci. Eng. A – Struct.* 109 (1989) 417–425.
- [22] P. Burzacchini, Porcelain tile, its history and development, *Ceram. World Rev.* 37 (2000) 96–103.
- [23] J. Martín-Márquez, J.M. Rincón, M. Romero, Effect of firing temperature on sintering of porcelain stoneware tiles, *Ceram. Int.* 34 (2008) 1867–1873.
- [24] F. Andreola, C. Siligardi, T. Manfredini, C. Carbonchi, Rheological behaviour and mechanical properties of porcelain stoneware bodies containing Italian clay added with bentonites, *Ceram. Int.* 35 (3) (2009) 1159–1164.
- [25] J. Martín-Márquez, A.G. de la Torre, M.A.G. Aranda, J.M. Rincón, M. Romero, Evolution with temperature of crystalline and amorphous phases in porcelain stoneware, *J. Am. Ceram. Soc.* 92 (1) (2009) 229–234.
- [26] S. Bribiesca, R. Equihua, L. Villaseñor, Photoacoustic thermal characterization of electrical porcelains: effect of alumina additions on thermal diffusivity and elastic constants, *J. Eur. Ceram. Soc.* 19 (1999) 1979–1985.
- [27] A. Michot, D.S. Smith, S. Degot, C.C. Gault, Thermal conductivity and specific heat of kaolinite: evolution with thermal treatment, *J. Eur. Ceram. Soc.* 28 (14) (2008) 2639–2644.
- [28] C. Efftinga, S. Güths, O.E. Alarcon, Evaluation of the thermal comfort of ceramic floor tiles, *Mater. Res.* 10 (3) (2007) 301–307.
- [29] L.M. Clark, R.E. Taylor, Radiation loss in the flash method for thermal diffusivity, *J. Appl. Phys.* 46 (2) (1975) 714–719.
- [30] C. Clauser, E. Huenges, Thermal conductivity of rocks and minerals, in: T.J. Ahrens (Ed.), *Rock Physics and Phase Relations*, AGU Reference Shelf 3, AGU, Washington, DC, 1995, pp. 105–126.
- [31] R. Barea, M.I. Osendi, J.M.F. Ferreira, P. Miranzo, Thermal conductivity of highly porous mullite material, *Acta Mater.* 53 (11) (2005) 3313–3318.
- [32] R. Barea, M. Belmonte, M.I. Osendi, P. Miranzo, Thermal conductivity of $\text{Al}_2\text{O}_3/\text{SiC}$ platelet composites, *J. Eur. Ceram. Soc.* 23 (11) (2003) 1773–1778.
- [33] W.D. Kingery, H.-K. Bowen, D.R. Uhlmann, *Introduction to ceramics*, 2nd ed., New York (NY), John Wiley & Sons, 1976.